2017 American Control Conference
Sheraton Seattle Hotel
May 24–26, 2017, Seattle, USA

Mosquito-Inspired Swarming for Decentralized Pursuit with Autonomous Vehicles

Daigo Shishika[1] and Derek A. Paley[2]

Abstract— **Inspired by the swarming behavior of male mosquitoes that aggregate to attract and subsequently pursue a female mosquito, we study how oscillatory motion in autonomous swarming vehicles helps the success of target capture. We consider the scenario in which multiple guardians with limited perceptual range are deployed to protect an area from an aerial intruder. The intruder becomes a target once it enters the perceptual range of a guardian and, when a guardian becomes a pursuer, it speeds up and chases the target. We focus on the strategy in the swarming phase, when the intruder has not yet been perceived by any of the guardians. In the parameter space consisting of the intruder's speed and guardians' ability (i.e., maximum acceleration and perceptual range) we identify necessary and sufficient conditions for target capture. We further compare circular and radial swarming motion and its effect on successful target capture. For the application to autonomous aerial vehicles, we propose a control algorithm that achieves swarming motion while also avoiding collisions. The theoretical results are demonstrated by experiments with a swarm of quadrotors.**

I. Introduction

The problem of pursuit has been studied in the context of missile guidance, robot control, animal behavior, and so on. Two ways we consider to categorize the existing work are by the objective (target intercept or capture/tracking) and by the strategy of the pursuer (cooperative or not). For missile guidance application, the goal of the pursuit is target *intercept*, where the pursuer aims to collide into the target [1]. Target intercept is also considered in pursuit-evasion games, where pursuit and evasion strategies have been studied with game-theoretic approaches [2][3]. A less aggressive pursuit scenario considered for the application to autonomous robots is target *capture*, where a pursuer seeks to approach and stay close to the target without colliding with it. A path-planning algorithm to capture a ground vehicle with a UAV is proposed in [4]. Strategies to encircle a target with a team of pursuers are proposed in [5][6]. In the work cited above, [2][5][6] describe cooperative strategies, whereas [1][4] are for a single pursuer.

Wild swarms of malarial mosquitoes [7][8] show an interesting combination of these categories. Male mosquitoes aggregate and form mating swarms to attract female mosquitoes that fly faster than the males. In this stage, which we call the *swarming phase*, male mosquitoes cooperate with one another to increase the chance of encounter with a female. When the female enters the swarm and the distance to one of the males becomes small (a *close encounter*), it triggers the male's pursuit behavior. In the *pursuit phase*, males compete against each other to capture the female. Therefore, their behavior is a combination of cooperative swarming and individual pursuit.

After the pursuit phase, the male and female exhibit coupling flight during which they fly in approximately the same direction while their separation distance oscillates—as though they are connected by a damped spring with zero rest length [9]. For a male to achieve this flight, simply intercepting a female is insufficient; he also has to align his velocity with the female. For this reason, the objective of the mosquito pursuit is a combination of target capture and intercept. Since the female flies faster than a swarming male, velocity alignment requires favorable initial conditions for the male, i.e., its initial velocity should be relatively aligned with female. This observation motivates our investigation below of swarming rather than static guardians.

Although the pursuit law that governs the motion of mosquitoes in the pursuit phase is an interesting topic, we focus on the swarming phase in this work. (See [10] for our previous work on pursuit.) A key characteristic of insect swarms is their unpolarized oscillatory motion [8], in contrast to fish schools [11], bird flocks [12], and formation controls inspired by those animals [13][14]. The oscillatory motion and the interactions between males have been previously studied [15], and it was suggested that this motion may increase the sensitivity to external stimuli, for example, to respond quickly to a female that enters the swarm [9][16].

Inspired by the mosquito behavior, we study how swarming motion may be useful in a scenario where multiple pursuers wait for a target that comes from an unknown direction at an unknown time. The goal of the pursuers is to capture the target, so simply blocking the target by constructing a wall-like formation will not achieve the goal. Instead, the pursuer has to align its velocity with the target.

The difficulty of achieving target capture depends on the capability of the pursuer (such as perceptual range and maximum acceleration) relative to the target's speed. We explore this parameter space to identify when the swarming motion is necessary for the pursuers' success. We further study what kind of swarming motion will increase the probability of successful pursuit. In addition, experiments using a small quadrotor testbed were conducted to validate the theoretical results. The experiments also highlight some of the challenges of real-life implementation, which improve

[1]Daigo Shishika is a graduate student in the Department of Aerospace Engineering, University of Maryland, 20742 MD College Park, USA daigo.shishika@gmail.com

[2]Derek A. Paley is the Willis H. Young Jr. Associate Professor of Aerospace Engineering Education in the Department of Aerospace Engineering and the Institute for Systems Research, University of Maryland, 20742 MD College Park, USA dpaley@umd.edu

978-1-5090-5994-2/$31.00 ©2017 AACC

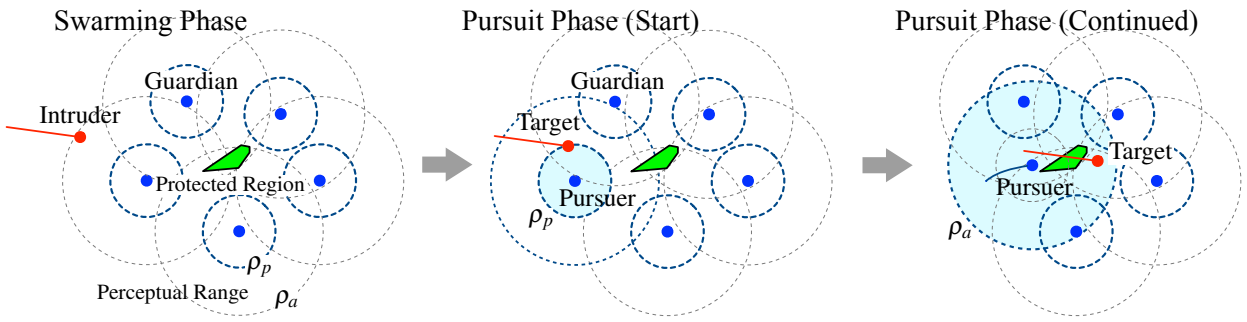

Fig. 1. Illustration of the swarming and pursuit scenario. In the swarming phase, an intruder (red) is approaching the protected region (green). The guardians (with static formation here for clarity) are deployed to wait for the intruder. Once the intruder enters the perceptual range, the guardian turns into a pursuer and pursues the target.

our swarming algorithm.

The contributions of this work are (1) identification of necessary and sufficient conditions related to guaranteed target capture; (2) analysis of how swarming behavior helps the pursuer's response to the target; (3) a control law that achieves swarming motion while also avoiding collisions; and (4) experimental demonstration of the control-theoretic results. The problem studied in this work can be applied to a situation where multiple vehicles are deployed to enforce a no-fly zone, for the application to drone countermeasures, or for convoy protection. The results of this work may provide a guideline in selecting the capabilities of the vehicles for such applications, and also provide a methodology to fully utilize those capabilities.

The paper outline is as follows. Section II formulates the problem. Section III presents the theoretical results. Section IV introduces the quadrotor testbed and describes the experimental results. Section V summarizes the paper and ongoing and future work.

II. Problem Formulation

Consider a planar system of point particles with unit mass representing N guardians and an intruder. The intruder seeks to pass through a protected region that is known to the guardians (see Fig. 1). However, the timing and the direction of the intruder trajectory is unknown. Once the intruder enters the perceptual range of the guardians, the roles of the agents change—the intruder becomes a target and the guardian becomes a pursuer. The goal of the pursuer is to capture the target (i.e., approach the target and stay close to it). Note that we do not distinguish between target capture before or after the intrusion.

We consider the case where the protected region is sufficiently small so that it can be approximated as a point O. Let O to be the origin of the inertial frame; $\boldsymbol{r}_i$, $\boldsymbol{v}_i$, and $\boldsymbol{a}_i$ denote the position, velocity, and acceleration of particle i in the inertial frame. The guardians have second-order dynamics, i.e., $\dot{\boldsymbol{r}}_i = \boldsymbol{v}_i$ and $\dot{\boldsymbol{v}}_i = \boldsymbol{a}_i$. To focus on the guardians' strategy, we assume that the intruder moves with a constant velocity $\|\boldsymbol{v}_T\| = v_T$ (we use the subscripts $_T$ and $_P$ to denote the intruder/target and guardian/pursuer, respectively). We also assume the following capabilities of the guardians:

(A1) Each guardian perceives the position and velocity of all other agents within the range ρ_a;

(A2) The identity (intruder or guardian) of the perceived agent is known only if it comes within the range $\rho_p < \rho_a$. This information is retained as long as it is in the range ρ_a; and

(A3) The magnitude of the guardian's acceleration is bounded according to $\|\boldsymbol{a}_P\| \le u_{\max}$.

In contrast to target *intercept* where pursuers aim to collide into the target, we consider target *capture*, which we define as follows.

Definition 1: Let $\boldsymbol{r}_{T/P} = \boldsymbol{r}_T - \boldsymbol{r}_P$ denote the relative position of the target with respect to the pursuer. Let $r_{\text{cap}} > 0$ denote the capture threshold. Target capture is successful if there exists t_{cap} such that $\|\boldsymbol{r}_{T/P}\| < r_{\text{cap}}$, for all $t > t_{\text{cap}}$.

The capture problem is separated into two parts. The first is the *swarming phase* in which the guardian does not know where the intruder is. Once the intruder enters the circle with radius ρ_p around the guardian, the *pursuit phase* starts. From assumption (A2), the pursuit phase can last as long as the target is in the range ρ_a. Therefore, we choose the threshold in Definition 1 to be $r_{\text{cap}} = \rho_a$.

Our main focus is on the swarming phase. The success of target capture depends on how quickly a guardian can respond (i.e., close the distance and align the velocity) to the intruder once it is in the perceptual range ρ_p. If the response is too slow, then the target will escape from the range ρ_a. We seek to find a strategy for how the guardians should prepare for the intruder to maximize the probability of target capture.

III. Theoretical Results

A. Limitation of Static Guardian

One possible strategy is to uniformly distribute stationary guardians around the protected area as in Fig. 1 and have them wait for the intruder. However, if the intruder is too fast, the guardian may not react (i.e., speed up) in time to keep the intruder in perceptual range. We first find the necessary condition for a static guardian to achieve target capture.

Proposition 1: A guardian who is stationary at the beginning of the pursuit phase never achieves target capture if

$$u_{\max} < \frac{v_T^2}{2(\rho_p + \rho_a)}. \tag{1}$$

Proof: Consider the easiest case for the pursuer: the target trajectory passes through the pursuer's position. Let $t_f = v_T/u_{\max}$ denote the time required for the pursuer to reach the speed v_T. The target escapes if it can travel a distance longer than $v_T t_f > \rho_p + \rho_a + \frac{1}{2}u_{\max}t_f^2$, which reduces to (1). ■

The above condition is given in terms of the intruder's speed v_T and the guardian's capability $u_{\max}$, ρ_a, and ρ_p. To explore this parameter space efficiently in the following sections, we introduce the following two nondimensional parameters:

$$\alpha = \frac{\rho_p}{\rho_a} \quad \text{and} \quad \Gamma = \frac{2u_{\max}(\rho_a + \rho_p)}{v_T^2}. \tag{2}$$

The first parameter $\alpha \in (0, 1]$ describes the ratio between the two perceptual ranges defined in assumptions (A1) and (A2). The second parameter Γ describes the ratio between the guardian's capability and the intruder's speed. Noting that Γ is obtained from the limiting case in (1), a static guardian will fail to capture a target if $\Gamma < 1$.

B. Sufficient Conditions for Target Capture

Next, we derive a sufficient condition for target capture. Since the condition will be given for the relative velocity $\boldsymbol{v}_{T/P}$ at the time of *close encounter* (i.e., the beginning of the pursuit phase), it applies to any guardian's strategy in the swarming phase. Based on this general condition, we consider two cases: a static swarm and a swarm with a circling motion.

As a pursuit law, $\boldsymbol{a}_P = \boldsymbol{F}_P^{(\text{pursuit})}$, following our previous work on mosquito-inspired swarm model [9], we consider a force resembling a damped-spring attached to the target, i.e.,

$$\boldsymbol{F}_P^1 = c\boldsymbol{r}_{T/P} + b\boldsymbol{v}_{T/P},$$

where c and b are positive constants. With the constraint

$$0 < c < u_{\max}/\rho_a, \tag{3}$$

the spring term alone never exceeds the acceleration limit $u_{\max}$. In this case, there always exists a scaling factor $\beta \in (0, 1]$ such that

$$\|c\boldsymbol{r}_{T/P} + \beta b\boldsymbol{v}_{T/P}\| \le u_{\max}. \tag{4}$$

In this way, the actual pursuit force is saturated as follows:

$$\begin{aligned} \boldsymbol{F}_P^{(\text{pursuit})} &= c\boldsymbol{r}_{T/P} + \beta b\boldsymbol{v}_{T/P}, \\ \beta &= \begin{cases} 1 & \text{if } \|c\boldsymbol{r}_{T/P} + b\boldsymbol{v}_{T/P}\| < u_{\max}, \\ \beta^* & \text{otherwise,} \end{cases} \end{aligned} \tag{5}$$

where $\beta^* > 0$ satisfies the equality in (4). (The value of β^* as a function of $\boldsymbol{r}_{T/P}$, $\boldsymbol{v}_{T/P}$, c and b can be obtained using Stewart's theorem in geometry, but it is omitted for brevity.) Although mosquitoes exhibit underdamped oscillation [9], for the application to guardians, a large number for b (i.e., over-damped spring) gives a good performance since velocity alignment is necessary for target capture. (Instability caused by the time delay also has to be taken into account for the gain tuning in practice.) However, the following proposition gives a sufficient condition for target capture, which is independent of the choice of c and b as long as (3) is satisfied.

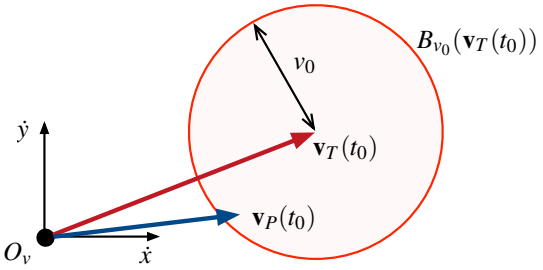

Fig. 2. Sufficient condition on the initial velocity for target capture depicted in the velocity space. Target capture is guaranteed if the pursuer's velocity (blue arrow) lies in the red circle at the beginning of the pursuit phase.

Proposition 2: Consider a pursuer under (5) with the gain c satisfying (3). Let t_0 denote the time when $\|\boldsymbol{r}_{T/P}\| = \rho_p$ (i.e., the time when the pursuit phase starts). The target capture is guaranteed if

$$\|\boldsymbol{v}_{T/P}(t_0)\| \le v_0, \quad \text{where} \quad v_0 = v_T\sqrt{\Gamma(1-\alpha)/2}. \tag{6}$$

Proof: Consider the energy function $V = \frac{1}{2}\|\boldsymbol{r}_{T/P}\|^2 + \frac{1}{2c}\|\boldsymbol{v}_{T/P}\|^2$. Since the target is not accelerating, the time derivative of V is

$$\begin{aligned} c\dot{V} &= c\boldsymbol{r}_{T/P}\cdot\boldsymbol{v}_{T/P} + \boldsymbol{v}_{T/P}\cdot(\boldsymbol{a}_T - \boldsymbol{a}_P) \\ &= c\boldsymbol{r}_{T/P}\cdot\boldsymbol{v}_{T/P} - \boldsymbol{v}_{T/P}\cdot(c\boldsymbol{r}_{T/P} + \beta b\boldsymbol{v}_{T/P}) \\ &= -\beta b\|\boldsymbol{v}_{T/P}\|^2. \end{aligned}$$

Thus, V is nonincreasing for all $t > t_0$. It follows that

$$\frac{1}{2}\|\boldsymbol{r}_{T/P}(t)\|^2 \le V(t) \le V(t_0) = \frac{1}{2}\rho_p^2 + \frac{1}{2c}\|\boldsymbol{v}_{T/P}(t_0)\|^2.$$

We obtain $\|\boldsymbol{r}_{T/P}(t)\| \le \rho_a$ for all $t > t_0$ if the right hand side of the above inequality is bounded by $\frac{1}{2}\rho_a^2$, i.e.,

$$\begin{aligned} \frac{1}{2}\rho_p^2 + \frac{1}{2c}\|\boldsymbol{v}_{T/P}(t_0)\|^2 &\le \frac{1}{2}\rho_a^2 \\ \|\boldsymbol{v}_{T/P}(t_0)\| &\le \sqrt{c(\rho_a^2 - \rho_p^2)} \end{aligned}$$

Noting that $\frac{u_{\max}}{\rho_a}(\rho_a^2 - \rho_p^2) = v_T^2\Gamma(1-\alpha)/2$ from the definition of Γ and α, the above inequality is equivalent to (6) with the constraint (3). ■

If the pursuer's velocity $\boldsymbol{v}_P(t_0)$ at the time of close encounter lies in the circle $B_{v_0}(\boldsymbol{v}_T(t_0)) \equiv \{\boldsymbol{v} | \|\boldsymbol{v} - \boldsymbol{v}_T(t_0)\| \le v_0\}$ centered at $\boldsymbol{v}_T(t_0)$ with radius v_0 (see Fig. 2), the target capture is guaranteed. If Γ is sufficiently large that the origin of the velocity space is included in $B_{v_0}(\boldsymbol{v}_T(t_0))$, even a static pursuer can guarantee target capture. This case is stated in the following result.

Corollary 1: Target capture is guaranteed by a pursuer who is stationary at the beginning of the pursuit phase if

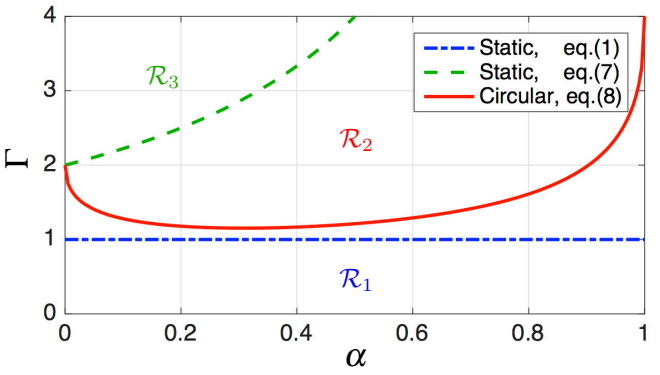

Fig. 3. Conditions for target capture in the nondimensional parameter space: $\mathcal{R}_1$ is where the static formation never achieves target capture; $\mathcal{R}_2$ is where target capture is guaranteed by circling formation; $\mathcal{R}_3$ is where the static formation guarantees target capture.

the following condition is satisfied:

$$\Gamma > 2/(1-\alpha). \tag{7}$$

Proof: From Proposition 2 and the discussion above, the sufficient condition is $v_0 > v_T$, which reduces to (7). ■

One strategy to achieve the velocity alignment derived in Proposition 2 is to use a circling motion. The target capture is guaranteed if the circling motion has (i) a radius less than ρ_p so that O is always in the perceptual range; (ii) sufficient speed such that $\|\boldsymbol{v}_P\| \in (v_T - v_0,\ v_T + v_0)$; and (iii) there are sufficiently many guardians so that there exists one whose direction of motion is approximately aligned with $\boldsymbol{v}_T$ when the intruder passes through O. Assuming (iii) is true, the conditions (i) and (ii) give the following result.

Corollary 2: Assuming that there are sufficiently many guardians so that there always exists one whose direction of motion is approximately aligned with $\boldsymbol{v}_T$, a circular motion in the swarming phase guarantees target capture if

$$\sqrt{\frac{\Gamma}{2}}\left(\sqrt{\frac{\alpha}{1+\alpha}} + \sqrt{1-\alpha}\right) > 1. \tag{8}$$

Proof: Given the smallest required speed $v_T - v_0$ and the acceleration bound $u_{\max}$, the radius of the circular orbit has to be greater than $(v_T - v_0)^2/u_{\max}$ to be able to counteract the centripetal acceleration. From condition (i), the radius also has to be smaller than ρ_p. Therefore, the condition is $\rho_p > (v_T - v_0)^2/u_{\max}$, which is equivalent to (8). ■

The analysis on the required number of guardians for condition (iii) alone to hold is omitted due to page constraints.

The necessary and sufficient conditions (1), (7) and (8) are summarized in Fig. 3. Region $\mathcal{R}_1$ is where a static swarm fails to achieve target capture. Region $\mathcal{R}_3$ is where a static swarm is guaranteed to achieve target capture, assuming that the intruder encounters at least one guardian. The region $\mathcal{R}_2 \cup \mathcal{R}_3$ is where a circling swarm is guaranteed to achieve target capture. The circling motion guarantees target capture with lower Γ as compared to a static swarm. If Γ is below the red curve in Fig. 3, guardians cannot achieve the desired circular motion; i.e., either the radius is too large or the speed is too low. The following section proposes strategies for the guardians so that they can achieve target capture even inside of the region $\mathcal{R}_1$.

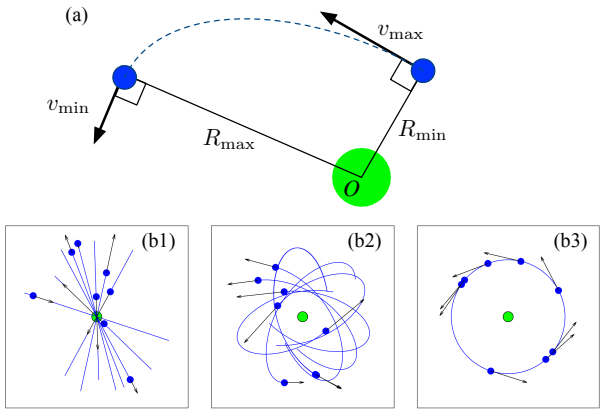

Fig. 4. Effect of initial conditions on the swarming motion. (a) The definition of $v_{\max}$ and $R_{\min}$; (b1) radial motion; (b2) general case; (b3) circular motion.

C. Swarming Motion and Probability of Target Capture

Consider a single guardian moving around O. A close encounter with an intruder occurs with probability $P_{\text{encounter}}$. At the time of the close encounter, condition (6) will hold only with probability P_{align}. The intruder will be captured if both of these two events happen for any one of the guardians in the swarm. (Explicit calculation of the probabilities $P_{\text{encounter}}$ and P_{align} is part of ongoing work.) Therefore, the two key objectives of the swarming motion are to (i) maintain high density around O where the intruder passes through; and (ii) maintain high speed that can lie in the circle $B_{v_0}(\boldsymbol{v}_T)$ defined after Proposition 2.

Let P_{capture} denote the probability that at least one pursuer captures the target. For the same number N of guardians, P_{capture} may be increased by improving $P_{\text{encounter}}$ and P_{align}, as discussed below.

Inspired by the swarming motion of male mosquitoes and existing work in the literature [8][15], we consider a central force $\boldsymbol{a}_i = \boldsymbol{F}_i^{(\text{center})}$ that generates oscillatory motion of the pursuers around O, where $\boldsymbol{F}_i^{(\text{center})} = -K_{\text{center}}\boldsymbol{r}_i$. Since the guardian's acceleration is bounded, the central force on agent i will be saturated as follows:

$$\boldsymbol{F}_i^{(\text{center})} = \begin{cases} -K_{\text{center}}\boldsymbol{r}_i & \text{if } \|K_{\text{center}}\boldsymbol{r}_i\| \le u_{\max}, \\ -u_{\max}\boldsymbol{r}_i/\|\boldsymbol{r}_i\| & \text{otherwise.} \end{cases} \tag{9}$$

For simplicity, consider the case where K_{center} is sufficiently large that $\boldsymbol{F}_i^{(\text{center})}$ is always saturated. Depending on the initial condition, the central force $\boldsymbol{F}_i^{(\text{center})}$ produces various orbiting motions characterized by the speed $v_{\max}$ and the distance from the center $R_{\min} \in [0, v_{\max}^2/u_{\max}]$ when the agent is closest to the center (see Fig. 4-(a)). Two extreme cases are (i) $R_{\min} = 0$, corresponding to a pure radial motion, and (ii) $R_{\min} = v_{\max}^2/u_{\max}$, corresponding to a pure circular motion. The set $(R_{\min}, v_{\max})$ not only affects the shape of the orbit, but also modulates the speed and the density of the

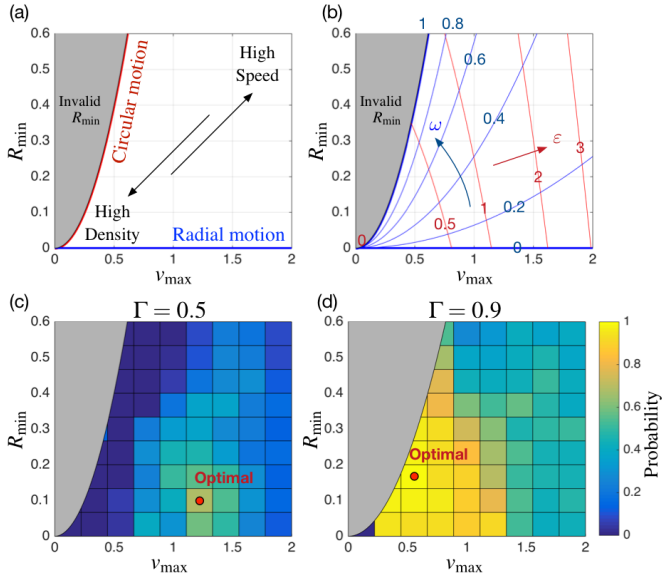

Fig. 5. Effect of swarming motion on the probability of target capture. The boundary of the gray region is where the motion is circular.

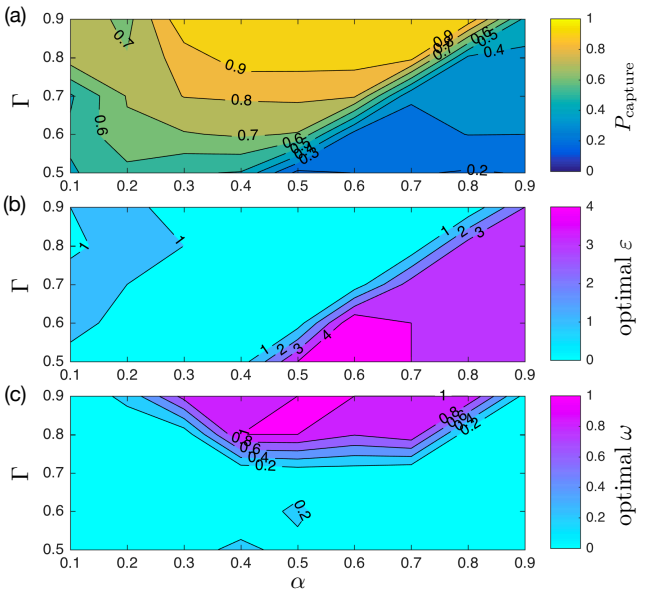

Fig. 6. Optimal orbiting motion as a function of system parameters Γ and α: (a) P_{capture} achieved with optimal orbiting motion; (b) optimal energy ε; (c) optimal roundness ω.

swarm. Figure 5-(c,d) shows P_{capture} obtained from numerical simulation with $N = 12$, $\alpha = 0.5$, and two values of Γ: 0.5 and 0.9. Although Γ is in region $\mathcal{R}_1$ for both cases, target capture is achieved with nonzero probability if the set $(R_{\min}, v_{\max})$ is chosen properly. Although the probability is higher with larger Γ, the optimal $(R_{\min}, v_{\max})$ varies with Γ. In particular, for $\Gamma = 0.5$, circling motion is not optimal; the probability of capture is maximized for a blended motion in Fig. 5-(b).

To further investigate how the optimal orbiting motion varies with Γ and α, two nondimensional parameters describe the energy and roundness of the orbits. Consider the following energy function:

$$E(v, \rho) = \frac{1}{2}v^2 + U(\rho), \tag{10}$$

where positive semidefinite function $U(\rho_p)$ denotes the potential energy. Since a large K_{center} so that $\|\boldsymbol{F}_i^{(\text{center})}\| = u_{\max}$ is assumed, we choose $U(\rho) = u_{\max}\rho$. Now, consider the baseline energy $E_0 = E(v_T - v_0, \rho_p)$ corresponding to the circling motion considered in Corollary 2. The nondimensional parameter $\varepsilon > 0$ describes the energy of the given orbit normalized by the baseline energy, i.e.,

$$\varepsilon \triangleq \frac{E(v_{\max}, R_{\min})}{E_0} = \frac{E(v_{\max}, R_{\min})}{E(v_T - v_0, \rho_p)}. \tag{11}$$

Remark 1: If K_{center} is sufficiently small so that $\boldsymbol{F}_i^{(\text{center})}$ is never saturated, then we choose $U(\rho) = \frac{K_{\text{center}}}{2}\rho^2$. For a general case we can use

$$U(\rho) = \begin{cases} \frac{K_{\text{center}}}{2}\rho^2 & \text{if } |\rho| < u_{\max}/K_{\text{center}}, \\ u_{\max}\left(\rho - \frac{u_{\max}}{2K_{\text{center}}}\right) & \text{otherwise.} \end{cases}$$

For the roundness of the orbit, consider the speed required to achieve a pure circular motion, i.e., $v^*_{\max} = \sqrt{u_{\max} R_{\min}}$. The nondimensional parameter $\omega \in [0, 1]$ defined by

$$\omega \triangleq \frac{v^*_{\max}}{v_{\max}} = \frac{\sqrt{u_{\max} R_{\min}}}{v_{\max}} \tag{12}$$

describes the degree of roundness scaled between 0 (pure radial motion) and 1 (pure circular motion). The level curves of ε and ω are depicted in Fig. 5-(b).

Remark 2: A point in $(v_{\max}, R_{\min})$-space is mapped to a unique point in (ε, ω)-space and vice versa through (11) and (12), except for the origin, which is mapped to the line $\varepsilon = 0$.

Figure 6 shows the optimal values of ε and ω as a function of the system parameters α and Γ. Figure 6-(b) shows that the swarm has to increase the energy for small Γ and large α. Since the energy is increased at the cost of swarm density (which causes a drop in $P_{\text{encounter}}$), we see low values of P_{capture} in the corresponding region in Fig. 6-(a). Figure 6-(c) shows that the pure circular motion is only optimal in the subset of the (α, Γ)-space.

Consider the case where guardian-vehicles have fixed values of α and $u_{\max}$, and intruders may have different speeds v_T that are approximately known a priori. For the guardians to respond optimally to different intruders (i.e., different Γ values), the swarm has to be able to change the orbiting motion between radial and circular. Motivated by the above observation, a control law that can modulate the balance between the radial and rotational component of the swarming motion is considered in the next section. In addition, collisions between the pursuers, which were ignored in the above analysis are taken into account for the actual implementation.

D. Swarming Control Law

We introduced $\boldsymbol{F}_i^{(\text{pursuit})}$ that generates a pursuit behavior in (5), and $\boldsymbol{F}_i^{(\text{center})}$ that generates oscillatory motion in (9).

This section introduces additional control terms to maintain the desired swarming motion in the experimental implementation. The final form of the control law consists of the following terms:

$$\begin{aligned} \boldsymbol{a}_i = \quad & (1-\lambda_i)\left(\boldsymbol{F}_i^{(\text{center})} + \boldsymbol{F}_i^{(\text{damp})} + \boldsymbol{F}_i^{(\text{angular})}\right) \\ & + \lambda_i \boldsymbol{F}_i^{(\text{pursuit})} + \boldsymbol{F}_i^{(\text{avoid})}. \end{aligned} \tag{13}$$

The switching function λ_i takes the value 0 when i is in the swarming phase and 1 when i is in the pursuit phase. The rule for this switching is described in Section II.

We use the following force for collision avoidance:

$$\boldsymbol{F}_i^{(\text{avoid})} = K_{\text{avoid}} \sum_{j \in S_i^{(\text{avoid})}} \frac{\boldsymbol{r}_{ij}}{\|\boldsymbol{r}_{ij}\|^2}, \tag{14}$$

where $S_i^{(\text{avoid})} = \{j \mid \|\boldsymbol{r}_{ij}\| < \rho_{\text{avoid}},\ \frac{d}{dt}\|\boldsymbol{r}_{ij}\| = \frac{\dot{\boldsymbol{r}}_{ij}\cdot\boldsymbol{r}_{ij}}{\|\boldsymbol{r}_{ij}\|} < 0\}$. Note, latency in the closed-loop system (see Section IV-A) causes delayed initiation and termination of avoidance. To alleviate the delay problem, the set $S_i^{(\text{avoid})}$ does not include the agents that are moving away from i. The damping term $\boldsymbol{F}_i^{(\text{damp})}$ is also introduced to avoid instability caused by the latency, i.e.,

$$\boldsymbol{F}_i^{(\text{damp})} = \begin{cases} -K_{\text{damp}}\dot{\boldsymbol{r}}_i & \text{if } \|\boldsymbol{r}_i\| > R_{\max}, \\ 0 & \text{otherwise.} \end{cases} \tag{15}$$

With the dissipation from $\boldsymbol{F}_i^{(\text{damp})}$ and the disturbance from $\boldsymbol{F}_i^{(\text{avoid})}$, the desired orbiting motion may not be maintained according to the analysis in the previous section. To ensure the circular component of the swarm, the angular momentum term $\boldsymbol{F}_i^{(\text{angular})}$ is introduced:

$$\boldsymbol{F}_i^{(\text{angular})} = h_{\text{des}}\boldsymbol{r}_i^{\perp}/\|\boldsymbol{r}_i\|^2 - \dot{\boldsymbol{r}}_i, \tag{16}$$

where $\boldsymbol{r}_i^{\perp}\cdot\boldsymbol{r}_i = 0$ and h_{des} is the desired angular momentum. The control gain h_{des} can be used together with K_{center} in (9) to determine the balance between the radial and circling motion of the agents.

In the experimental implementation, a radial motion like Fig. 4-(b1) is difficult to achieve when the vehicle size is sufficiently large relative to the spatial size of the swarm, since the risk of collision is high at the center. Also, the shape of the orbiting motion is distorted due to the force from collision avoidance. For these reasons, direct extension of the parameters ε and ω into the swarming algorithm is challenging, and is a subject of ongoing and future work.

IV. Experimental Testbed and Results

A. Quadrotor Testbed

We conducted experiments using a group of small-size quadrotors in an indoor motion-capture environment. We used five BLADE Nano QX, which is a commercially available quadrotor. The architecture of the experiments is summarized in Fig. 7. The commands are computed on a desktop computer and sent to an Arduino Nano via USB serial communication. The Arduino Nano converts the received serial signal into a PPM (Pulse Position Modulation) command and sends it to the trainer port of a Spektrum DX6 transmitter which sends RF (Radio Frequency) commands to the vehicle. The OptiTrack motion-capture system tracks the position and attitude of the vehicle and streams them to the computer. When it is sent out from the computer, the control law proposed in Section III-D is converted to a desired stick input [17].

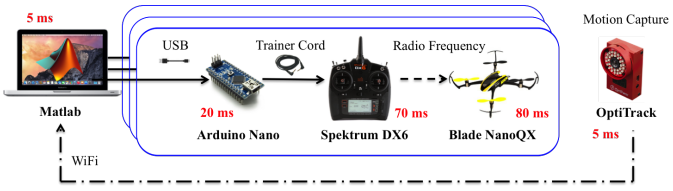

Fig. 7. The architecture of the experimental setup. The red numbers indicate the approximate time delay from each component. The blue box is duplicated according to the number of vehicles.

One limitation of our experimental setup is the time delay (approximately 170 ms) between the Arduino Nano and the Nano QX. Another limitation is the size of the test area. The vehicle dimension is 18.2×18.2×6.4 cm, whereas the horizontal area of the volume tracked by the motion-capture system is approximately 3×3 m. To maintain a swarming motion with sufficiently high speed in this confined area, collision avoidance is an important consideration.

B. Swarming Phase

First, we show how five vehicles successfully achieve swarming with the decentralized algorithm proposed in Section III-D. Since the sensing is done with motion-capture system, we simulate the effect of limited perceptual range. The parameters K_{avoid}=3.0 and ρ_{avoid}=2.0 m were chosen sufficiently large to achieve collision avoidance. The parameter h_{des} in (16) was varied in real time to modulate the speed of the vehicles. Although $u_{\max}$ defined in (A3) denoted the limitation of the vehicle in the theoretical analysis, we vary it as a control parameter for the term $\boldsymbol{F}_i^{(\text{center})}$ in the experiment. We chose $u_{\max} = 1 + 0.6|h_{\text{des}}|$ and $K_{\text{center}} = 20$. Figure 8-(a) shows a snapshot of the swarming reconstructed from motion-capture data. The tails show the trajectories from the last 5 seconds. Figure 8-(b) shows how the absolute value $|h_{\text{des}}|$ can be used to control the tangential speed of the vehicles to modulate the balance between the radial and rotational component of the swarming motion. (The sign of h_{des} determines the direction of rotation.)

C. Pursuit Phase

Next, we show the effect of swarming motion on the success of pursuit. Because of the spatial constraints, we used one guardian and a fictitious intruder simulated in computer. The maximum acceleration of the vehicle is approximately $u_{\max} = 6.0\ \text{ms}^{-2}$. (Note that this is the limit as is defined in (A3).) By varying v_T, we experimentally tested pursuit with different values of Γ. For a static guardian with $\alpha = 0.67$, where $\rho_a = 0.6$ m and $\rho_p = 0.4$ m, we simulated the easiest-case scenario considered in the proof of Proposition 1, i.e., the case where the intruder's trajectory passes through the guardian's position. Although the theory predicts that

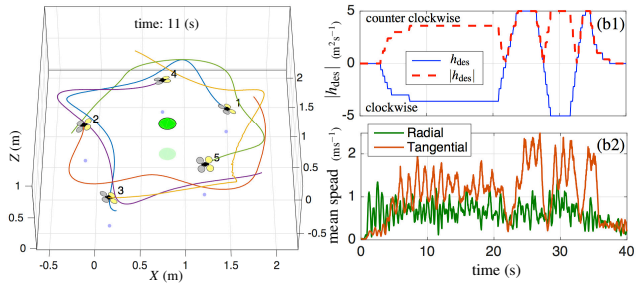

Fig. 8. (a) Snapshot of the swarming. Position and attitude of the vehicles are obtained from motion-capture system. The animation is available at [*https://youtu.be/Hova4bMiVZg*]; (b1) the control gain $h_{\rm des}$ that modulates the balance between the radial and rotational motion; (b2) time history of the radial and tangential speed averaged over five vehicles. The tangential speed follows the magnitude of $h_{\rm des}$

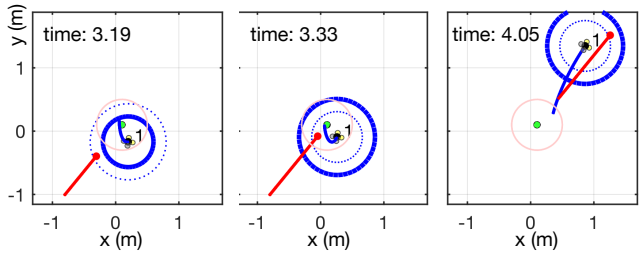

Fig. 9. Snapshot of the pursuit phase reconstructed from motion-capture data. The relevant perceptual range changes from ρ_p to ρ_a between the first two figures.

$\Gamma > 1$ will enable target capture for this easiest case, in the experiment, we required $\Gamma > 1.78$ (or equivalently $v_T < 2.6$ ms^{-1}) due to the latency in the system.

For the swarming case, we further increased the intruder's speed to $v_T = 2.9$ ms^{-1}, which corresponds to $\Gamma = 1.43$. Although Γ is decreased by 20%, target capture was successful in 6 out of 21 trials, which gives $P_{\rm capture} = 0.29$. (Note that a static guardian achieve $P_{\rm capture} = 0$ for this value of Γ.) Figure 9 shows the snapshot of the vehicle transitioning from swarming to pursuit, and maintaining the target in the perceptual range.

V. Conclusions

This paper describes a swarming strategy for multiple guardians to defend a protected zone from an intruder. A static guardian requires high capability to guarantee target capture, whereas swarming motion relaxes the requirement. Using radial oscillatory motion, guardians with arbitrarily low capability achieve target capture with some probability by utilizing the velocity alignment that occurs by chance. Guardians should compromise between the swarm density and their speed to increase the probability of target capture.

A decentralized control algorithm that achieves collision avoidance while maintaining a desired circular motion was proposed and tested with a quadrotor testbed. The algorithm successfully generated a swarm in the presence of time delay. The experiment also validated that a swarming motion helps the guardians to capture the intruder.

In ongoing and future work, we are extending the swarming algorithm to three dimensions, which involves the avoidance of the downwash from other vehicles. With inspiration from mosquito swarms, we are investigating how the velocity alignment behavior between the guardians (which occurs before target detection) will improve the probability of successful pursuit. We are also studying the case where there can be multiple intruders that are performing evasive strategies.

ACKNOWLEDGMENT

The authors would like to acknowledge valuable discussions with Nicholas Manoukis and Sachit Butail related to the behavior of mosquitoes, and also the support from Derrick Yoe related to the experimental testbed.

References

[1] P. Zarchan, *Tactical and Strategic Missile Guidance*. Washington, DC, USA: AIAA, 2002, vol. 176.

[2] A. Antoniades, H. J. Kim, and S. Sastry, "Pursuit-evasion strategies for teams of multiple agents with incomplete information," *42nd IEEE Conf. Decision Control (CDC)*, pp. 756–761, 2003.

[3] J. Selvakumar and B. Efstathios, "Evasion from a group of pursuers with a prescribed target set for the evader," *Proc. Amer. Control Conf. (ACC)*, pp. 4–9, 2016.

[4] J. Lee, R. Huang, A. Vaughn, and X. Xiao, "Strategies of path-planning for a UAV to track a ground vehicle," *AINS Conf.*, 2003.

[5] T. H. Kim and T. Sugie, "Cooperative control for target-capturing task based on a cyclic pursuit strategy," *Automatica*, vol. 43, no. 8, pp. 1426–1431, 2007.

[6] S. D. Bopardikar, F. Bullo, and J. P. Hespanha, "A cooperative homicidal chauffeur game," *Automatica*, vol. 45, no. 7, pp. 1771–1777, 2009.

[7] N. C. Manoukis, A. Diabate, A. Abdoulaye, M. Diallo, A. Dao, J. M. Ribeiro, and T. Lehmann, "Structure and dynamics of male swarms of *Anopheles gambiae*." *J. Med. Entomol.*, vol. 46, no. 2, pp. 227–235, 2009.

[8] S. Butail, N. Manoukis, and M. Diallo, "The dance of male *anopheles gambiae* in wild mating swarms," *J. Med. Entomol.*, vol. 50, no. 3, pp. 552–559, 2013.

[9] D. Shishika and D. Paley, "Lyapunov stability analysis of a mosquito-inspired swarm model," *54th IEEE Conf. Decision Control (CDC)*, 2015, pp. 482–488.

[10] D. Shishika, J. K. Yim, and D. A. Paley, "Robust Lyapunov control design for bioinspired pursuit with autonomous hovercraft," *IEEE Trans. Control Syst. Technol.*, no. 99, pp. 1–12, 2016.

[11] C. Becco, N. Vandewalle, J. Delcourt, and P. Poncin, "Experimental evidences of a structural and dynamical transition in fish school," *Physica A*, vol. 367, pp. 487–493, jul 2006.

[12] A. Cavagna, A. Cimarelli, I. Giardina, G. Parisi, R. Santagati, F. Stefanini, and M. Viale, "Scale-free correlations in starling flocks," *Proc. Natl. Acad. Sci. U.S.A.*, vol. 107, no. 26, pp. 11865-11870, June 2010.

[13] R. Olfati-Saber and R. Murray, "Flocking with obstacle avoidance: cooperation with limited information in mobile networks," *42nd IEEE Conf. Decision Control (CDC)*, vol. 2, no. December, pp. 2022–2028, 2003.

[14] A. Levant, "Flocking for multi-agent dynamic systems: Algorithms and theory," *IEEE Trans. Autom. Control*, vol. 51, pp. 1–20, 2006.

[15] D. Shishika, N. Manoukis, S. Butail, and D. Paley, "Male motion coordination in anopheline mating swarms," *Sci. Rep.*, vol. 4, pp. 1–7, 2014.

[16] A. Attanasi, A. Cavagna, L. Del Castello, I. Giardina, S. Melillo, L. Parisi, O. Pohl, B. Rossaro, E. Shen, E. Silvestri, and M. Viale, "Collective behaviour without collective order in wild swarms of midges," *PLoS Comput. Biol.*, vol. 10, no. 7, pp. 1–10, 2014.

[17] Z. Zuo, "Trajectory tracking control design with command-filtered compensation for a quadrotor," *IET Control Theory Appl.*, vol. 4, no. 11, pp. 2343–2355, 2010.